# Wave Packet Dynamics in a Quasi-One-Dimensional Metal-Halogen Complex Studied by Ultrafast Time-Resolved Spectroscopy

A. Sugita, T. Saito, and H. Kano
*Department of Physics, University of Tokyo, 7-3-1, Hongo, Bukyo-ku, Tokyo 113-0033, Japan*

M. Yamashita
*Department of Chemistry, Tokyo Metropolitan University, Hachioji, Tokyo 192-0397, Japan*

T. Kobayashi
*Department of Physics, University of Tokyo, 7-3-1, Hongo, Bukyo-ku, Tokyo 113-0033, Japan*
(Received 14 June 2000)

An ultrafast optical response is studied in a quasi-one-dimensional halogen-bridged mixed-valence metal complex $[Pt(en)_2][Pt(en)_2I_2](ClO_4)_4$ with ultrafast time resolution. Wave packet motions both in the ground and self-trapped exciton (STE) states are observed as oscillatory modulations in the time-resolved reflectivity. The wave packet motion on the STE potential surface begins after about 50 fs with respect to the photoexcitation. This delay is attributed to the lattice relaxation from the free exciton state to the STE state.

DOI: 10.1103/PhysRevLett.86.2158 PACS numbers: 78.47.+p, 71.35.Cc, 71.38.–k, 71.45.Lr

The spectroscopic properties of excitons in many-electron systems of insulators, alkali halides, or organic molecular crystals have been attracting a lot of interest [1,2]. Among them, one-dimensional (1D) exciton systems show the specific features which are not found in two- or three-dimensional (2 or 3D) exciton systems [3–5]. Because of the transfer of electrons and holes between different atomic sites, the exciton is highly delocalized, as opposed to the case of localized excitations in isolated molecular systems. An electron-phonon (e-ph) interaction, which also plays an important role in the excitonic properties, is closely related to the radius of the exciton in the materials [6]. When the transfer energy is large and the e-ph interaction energy is small, the exciton extends over many atomic sites and the radius is large. This exciton state is called a free exciton (FE) state. On the other hand, when the electron-phonon interaction energy is comparable to or larger than the transfer energy, the FE is not the only stable exciton state. In this case, the exciton deforms the surrounding lattice configurations and is trapped by this deformed potential. In this self-trapped exciton (STE) state, the exciton wave function is limited in a volume of a small Bohr radius. Even in the latter system characterized by the large e-ph interaction energy, however, the primary photoexcited state is the FE state, and the lattice deformation later traps the exciton in its potential. Especially 1D exciton systems were shown theoretically to have a peculiarity with no potential barrier between the FE and the STE states. This feature is expected to show quite different dynamics from those of the 2 or 3D exciton systems [7].

Quasi-one-dimensional halogen-bridged mixed-valence metal complexes (HMMCs) are grouped in a charge-transfer exciton system with a strong e-ph interaction [6]. The main structure of HMMCs is described as $\cdots M^{2+} \cdots X^{-}$—$M^{4+}$—$X^{-} \cdots M^{2+} \cdots X^{-}$, where M and X are a transition metal ion and bridged-halogen ion, respectively. The unbalance of the charge distribution between $M^{4+}$ and $M^{2+}$ is the consequence of a Peierls instability. The $X^{-}$ is shifted from the center of the neighboring metal sites and is located closer to $M^{4+}$. The peak energy of the luminescence spectrum is almost half of the peak energy of the exciton band [8]. This large Stokes shift indicates the large e-ph interaction. Higher order overtones up to the 21st are observed in a resonant Raman scattering experiment [8], which suggests that the potential surface can be approximated by a harmonic potential. Therefore, the HMMC systems satisfy an ideal 1D exciton model with a large e-ph interaction energy.

In this Letter, we studied the ultrafast optical response of the HMMC and observed the oscillatory signal attributed to the wave packets coherently driven by a short optical pulse. The dynamics of the wave packets both in the electronic ground and excited states is discussed. The wave packet dynamics of the STE state was reported in the previous papers [9,10]. However, the time resolution was not short enough to determine unambiguously the phase of the wave packet, which gives the important information about the primary dynamics of the photoexcited state. In the present work, the time resolution better than 5 fs enables us to determine the vibrational phase very precisely and to discuss the ultrafast lattice relaxation process from FE to STE.

Time-resolved reflectivity is measured by pump and probe spectroscopy. An ultrashort light pulse is generated by a pulse-front matched noncollinearly phase-matched optical parametric amplifer [11]. The broad amplified spectrum extends from 550 to 750 nm. The pulse energy is about 7 $\mu$J. The cross correlation width of the pump and probe pulse is 7 fs. The sample is a single crystal of $[Pt(en)_2][Pt(en)_2I_2](ClO_4)_4$ (en = ethylenediamine),

 0031-9007/01/86(10)/2158(4)$15.00 © 2001 The American Physical Society

abbreviated as Pt-I in the following. The polarizations of the pump and probe are both parallel to the orientation of the MX chain. All the experiments were done at 293 K. The peak energy of the exciton band of Pt-I is 1.38 eV which means that the spectrum of the excitation light covers higher levels in the exciton band.

Figures 1(a) and 2(a) show the time-resolved reflectivity $[(\Delta R/R)_{\text{exp}}]$ at 2.00 and 1.77 eV, respectively. A negative reflectivity change is observed, and an oscillatory contribution is superimposed on it. The slowly varying signal $[(\Delta R/R)_{\text{slow}}]$ is reproduced with an equation,

$$\left(\frac{\Delta R}{R}\right)_{\text{slow}} = a\exp\left(-\frac{t}{\tau_1}\right) + b - (a+b)\exp\left(-\frac{t}{\tau_2}\right). \quad (1)$$

The parameters are determined as $\tau_1 = 1.4 \pm 0.1$ ps and $\tau_2 = 130 \pm 20$ fs at 2.00 eV and $\tau_1 = 1.4 \pm 0.1$ ps and $\tau_2 = 150 \pm 20$ fs at 1.77 eV, respectively. In our previous work on $[\text{Pt(en)}_2][\text{Pt(en)}_2\text{Cl}_2](\text{ClO}_4)_4$, the dynamics of the STE was studied by pump and probe spectroscopy [12]. The nonequilibrated STE is thermalized within about 1 ps. Then, the thermalized STE recovers to the ground state within about 90 ps. This mechanism was supported by time-resolved emission spectroscopy [13]. In accordance with these results, the $\tau_1$ decay and constant components in Eq. (1) are attributed to the nonequilibrated and equilibrated STEs, respectively. Recently, the transient absorption was studied in $[\text{Pt(en)}_2][\text{Pt(en)}_2\text{Br}_2](\text{PF}_6)_4$ [10]. The rise time of about 200 fs, which reflects the formation of the nonthermal STE, is correspondent with the time constant $\tau_2 \sim 150$ fs in the present study.

Figures 1(b) and 2(b) show the contribution of the oscillatory component which is equal to the difference between two components, $(\Delta R/R)_{\text{osc}} = (\Delta R/R)_{\text{exp}} - (\Delta R/R)_{\text{slow}}$. The $(\Delta R/R)_{\text{osc}}$ is converted to a frequency spectrum by fast Fourier transformation (FFT), and the spectrum is shown in Figs. 1(c) and 2(c). The resolution of the FFT spectrum is $\pm 3$ cm$^{-1}$. At 2.00 eV, the FFT spectrum has two peaks at 107 and 124 cm$^{-1}$. The peak at 124 cm$^{-1}$ is almost equal to the frequency of the symmetric stretching ($\text{I}^{-1}$—$\text{M}^{4+}$—$\text{I}^{-1}$) mode at 122.6 cm$^{-1}$ observed in resonant Raman spectrum [14]. The temporal profile of $(\Delta R/R)_{\text{osc}}$ is expressed by the summation of two differently damped oscillations as

$$\left(\frac{\Delta R}{R}\right)_{\text{osc}} = A\exp\left(-\frac{t}{\tau_A}\right)\cos\left(2\pi\,\frac{t}{T_A} - \theta_A\right) + B\exp\left(-\frac{t}{\tau_B}\right)\cos\left(2\pi\,\frac{t}{T_B} - \theta_B\right). \quad (2)$$

The oscillation periods of $T_A = 310$ fs and $T_B = 270$ fs, which correspond to the frequencies at 107 and 124 cm$^{-1}$ respectively, are used in the least squares fitting. The parameters are evaluated as $\tau_A = 290 \pm 10$ fs, $\theta_A = 240° \pm 6°$, $\tau_B = 1.1 \pm 0.1$ ps, $\theta_B = -85° \pm 6°$. On the other hand, at the probe energy of 1.77 eV, there is only one peak observed at 110 cm$^{-1}$, and the higher frequency peak around 123 cm$^{-1}$ is not found. The

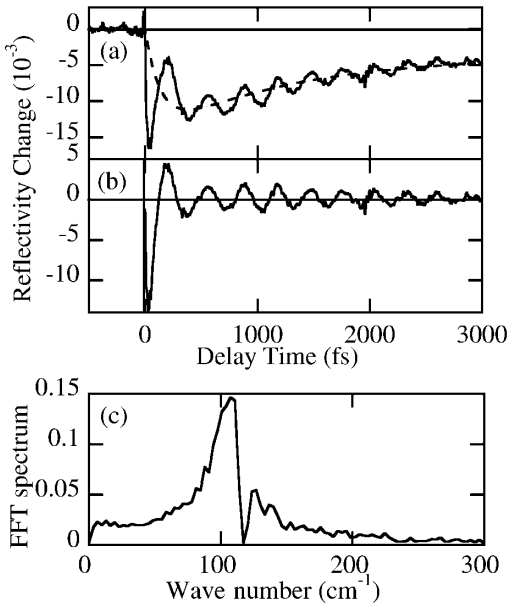


FIG. 1. (a) Time-resolved reflectivity change $(\Delta R/R)_{\text{exp}}$ of Pt-I at the probe energy 2.00 eV (solid curve). The dashed curve is the contribution of the slowly varying component $(\Delta R/R)_{\text{slow}}$ described by Eq. (1). (b) The oscillatory component extracted from the time dependent data (a), which corresponds to the difference $(\Delta R/R)_{\text{osc}} = (\Delta R/R)_{\text{exp}} - (\Delta R/R)_{\text{slow}}$. (c) The Fourier spectrum of the oscillatory component $(\Delta R/R)$.

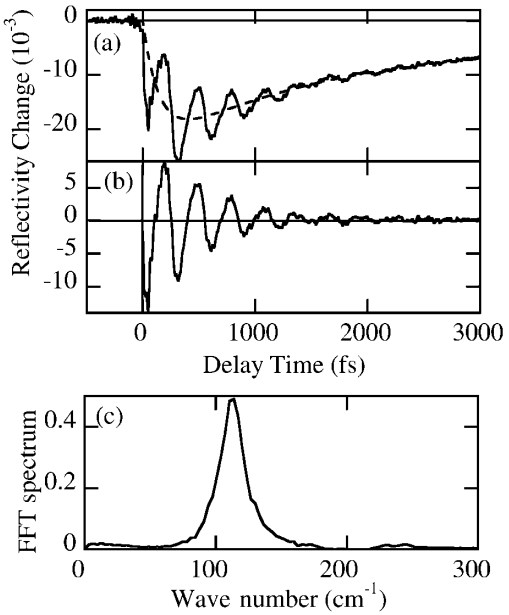


FIG. 2. Time-resolved reflectivity change $(\Delta R/R)_{\text{exp}}$ of Pt-I at the probe energy 1.77 eV (solid curve). The dashed curve is the contribution of the slowly varying component $(\Delta R/R)_{\text{slow}}$ described by Eq. (1). (b) The oscillatory component extracted from the time dependent data (a), which corresponds to the difference $(\Delta R/R)_{\text{osc}} = (\Delta R/R)_{\text{exp}} - (\Delta R/R)_{\text{slow}}$. (c) The Fourier spectrum of the oscillatory component $(\Delta R/R)$.

oscillatory signal is reproduced with a single damped oscillation as

$$\left(\frac{\Delta R}{R}\right)_{\text{osc}} = A\exp\left(-\frac{t}{\tau_A}\right)\cos\left(2\pi\,\frac{t}{T_A} - \theta_A\right). \quad (3)$$

The parameters are evaluated as $\tau_A = 590 \pm 10$ fs and $\theta_A = 225° \pm 5°$ with the oscillation period $T_A = 300$ fs estimated from the peak frequency of the FFT spectrum.

The parameters $\tau_A$ and $\tau_B$ consist of two contributions, that is, the dephasing rates of the wave packet $k_A$ and $k_B$ and the population relaxation of the nonthermal STE, $\tau_1 = 1.4$ ps. These parameters are related by $\tau_A^{-1} = k_A + \tau_1^{-1}$ and $\tau_B^{-1} = k_B + \tau_1^{-1}$. Figure 3 shows the dephasing rates $k_A$ and $k_B$ and the phases $\theta_A$ and $\theta_B$ against probe energy. The rapidly damped oscillation $A$ is found in the entire probe energy region studied in the present study, and the $k_A$ is closely dependent on the probe energy. On the other hand, the slowly damped oscillation $B$ is observed at the probe energy larger than 1.88 eV, and the $k_B$ is nearly constant within the probe energy where it is observed. The formation of the wave packet can be realized both in the electronic ground and excited states. Judging from the dephasing rates of $k_A$ and $k_B$, the rapidly damped component with the oscillation frequency of 122 $\text{cm}^{-1}$ is attributed to the wave packet motion in the electronic excited state, while the slowly damped one with the frequency of 110 $\text{cm}^{-1}$ is attributed to the motion in the electronic ground (G) state.

The wave packet dynamics in the STE potential is discussed. As has been seen in Fig. 3(a), the $k_A$ is dependent on the probe energy, and it decreases monotonously with the probe energy from 1.77 to 2.00 eV. This probe energy dependence reflects the thermalization process in the STE potential. Because of the strong e-ph interaction, the STE have a large amount of excess vibrational energy just after the lattice relaxation from the FE state. Assuming that the potentials of the ground and STE states are harmonic, the excess energy is estimated to be 1.0 eV, which is determined from the excitation energy $E_{\text{ex}} = 2.0$ eV, the peak energy of the stationary absorption $E_1 = 1.4$ eV, and the stationary emission $E_2 = 0.6$ eV [15]. The nonthermal STE should dissipate this excess energy to the surrounding heat bath, relaxing from higher to lower vibrational excited levels. Accordingly, the amplitude of the vibration decreases with the delay time, and the transient absorption is probable only from the lower levels of the vibrational excited states close to the bottom of the STE potential. Hence, the larger (smaller) value of $k_A$ observed at higher (lower) probe energy is attributed to the transient absorption from higher (lower) vibrational excited levels in the STE potential surface.

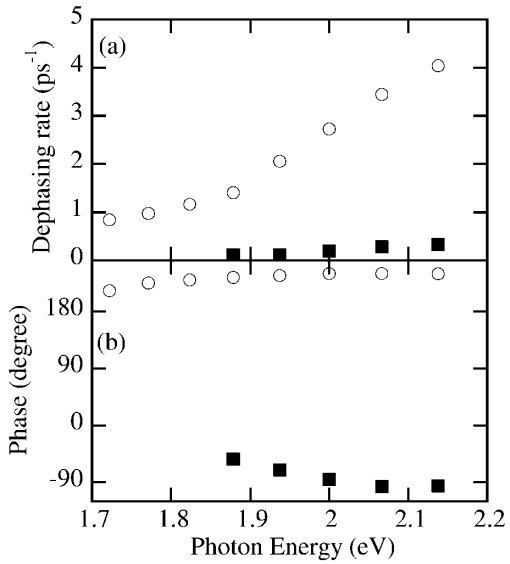


FIG. 3. (a) Probe energy dependence of the dephasing rates $k_A$ (open circles) and $k_B$ (filled squares) in Eqs. (2) and (3). (b) Probe energy dependence of the phases $\theta_A$ (open circles) and $\theta_B$ (filled squares) in Eqs. (2) and (3).

The wave packet motion in the electronic excited state starts in the Franck-Condon region, and it propagates to the outer turning point by way of the bottom of the STE potential. As can be seen in Fig. 2(b), the onset of the observed oscillatory signal begins at the minimum intensity, and it gradually increases to the maximum intensity. Hence, in the present probe energy, the wave packet motion becomes closer to the electronic resonance, as it approaches the outer turning point. Thus, the observed photoinduced absorption signal should be transition from the vibrational coordinate close to the outer turning point. In the isolated molecular system, the phase of the oscillation is expected to be 180° for the absorption from the vibrational coordinate close to the outer turning point. However, the observed phase $\theta_A \sim 240°$ is deviated from 180° at the whole probe energy region. The deviation is much larger than the accuracy of the phase $\pm 6°$, which corresponds to 5 fs time resolution of the present spectrometer. Therefore, the wave packet motion of the STE is delayed substantially at the onset of the oscillation with respect to the photoexcitation. The interval time is estimated to be about 50 fs ($= T_A \times \frac{60°}{360°}$) between the photoexcitation and the onset of the wave packet motion.

The formation and transport properties of the STE are determined by the transfer energy as well as the e-ph interaction energy. This is different from the case of the wave packet generated in the isolated molecular system where only the e-ph interaction energy determines the wave packet dynamics. The initial photoexcited state is the FE state, and the exciton is considered to be delocalized over many different sites. The FE and STE potential surfaces are expected to be continuous and, furthermore, as a characteristic of the 1D exciton system, there is no potential barrier between FE and STE potential surfaces [7]. Consequently, the lattice relaxation process from the FE to STE states begins to take place spontaneously just after its formation (Fig. 4).

The potential is considered to be anharmonic in the boundary region between the FE and STE potentials, while

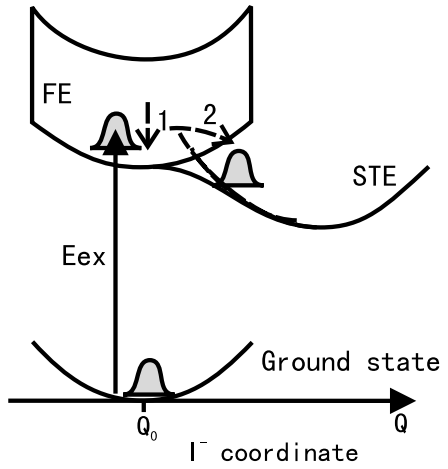


FIG. 4. Model of the relaxation dynamics and potential of the exciton in Pt-I. Arrows 1 and 2 denote the thermalization process in the FE band and the lattice relaxation from FE to STE states, respectively.

the STE potential is well approximated to be harmonic in the lower vibrational excited levels. The STE potential is connected to the bottom of the FE band without a barrier, and hence the curvature of the potential is expected to be flat in this region. Therefore, the atom is not accelerated by the potential force at the onset of the wave packet motion, which results in the delay of the phase $\theta_A$. In other words, the delay time is related to the time required for the shrinkage of the exciton radius from the FE to STE state, resulting in the exciton coupling more tightly with specific sites after the lattice relaxation process. Once the exciton is trapped by the harmonic potential of the STE, the wave packet starts the vibration and the motion of the $I^-$ can be approximated to the damped oscillation. The excitation energy used in the present study is higher than the peak of the FE band by about 0.6 eV, and the thermalization within the band is also expected to take place. Therefore, the delay time of the onset of the wave packet motion gives an upper limit of the lattice relaxation process between the FE and STE states.

A noticeable point is the conservation of the vibrational coherence of the wave packet motion between the FE and STE states during the lattice relaxation. Since the excitation light pulse has a broadband spectrum, the excitons are distributed over many different levels in the FE band just after the photoexcitation. These excitons have different relaxation paths, which can be the cause of dephasing the coherence of the wave packet. The time required for the lattice relaxation is found to be about 50 fs, which is much shorter than the oscillation period of 300 fs. Hence it is reasonable that the coherence still remains after the lattice relaxation.

Next, the wave packet motion in the G state is to be discussed. The shape of the Raman spectrum is closely related to the depasing process of the wave packet in the G state. When the spectrum is Lorentzian, that is, $I_{\mathrm{RS}} \propto \frac{\Gamma}{(\nu-\nu_0)^2+\Gamma^2}$ with frequency $\nu$, the coherence of the wave packet is expected to dephase exponentially with a decay constant of $2\Gamma$, which is expressed by the summation of the pure dephasing and population decay rates of the vibrational excited levels in the electronic ground state [16]. Here, the parameters $\nu_0$ and $2\Gamma$ are the center frequency of the Raman mode and its linewidth. In Pt-I, the linewidth of the $I^-$—$Pt^{4+}$—$I^-$ stretching mode is reported to be $2\Gamma = 10\ \mathrm{cm}^{-1}$ [14]. Meanwhile, the dephasing rate of the wave packet motion in the G state is determined experimentally to be $k_B = (2.0 \pm 0.5) \times 10^{-1}\ \mathrm{ps}^{-1}$, and it is correspondent to the frequency width of $2\Gamma_{\mathrm{exp}} = k_B/c = 7 \pm 2\ \mathrm{cm}^{-1}$. These values are in fairly good agreement within the experimental error. The phase $\theta_B$ is close to $-90°$ in the entire probe energy region, which means that the oscillation of the wave packet is sinelike. This sinelike oscillation is well consistent with the expectation of an impulsive stimulated Raman scattering (ISRS) mechanism which is proposed for the formation of the wave packet on the G state [17].

In conclusion, the wave packet motions in the STE and the electronic ground states are studied in Pt-I with an ultrafast time-resolved spectroscopy. The formation mechanism of the wave packet on the G state is explained by the ISRS mechanism. On the other hand, the beginning of the wave packet motion in the STE state is delayed by about 50 fs with respect to the photoexcitation. The delay time is attributed to the lattice relaxation process between the FE and STE states and the thermalization process in the FE band.

This work is supported by Research for the Future (RFTF) of Japan Society for the Promotion of Science. The authors thank Satoshi Tanaka, Holger F. Hofmann, and Naoki Fukutake for fruitful discussions.

[1] M. Ueta *et al., Excitonic Processes in Solids* (Springer-Verlag, Berlin, 1986), p. 203.
[2] E. I. Rashba, *Excitons* (North-Holland, Amsterdam, 1987), p. 273.
[3] T. Kobayashi, *Relaxation in Polymers* (World Scientific, Singapore, 1993).
[4] T. Kobayashi, *J-Aggregate* (World Scientific, Singapore, 1996).
[5] T. Kobayashi *et al.,* J. Opt. Soc. Am. B **7**, 1558 (1990).
[6] K. S. Song *et al., Self-Trapped Excitons* (Springer-Verlag, Berlin, 1996), p. 369.
[7] Y. Toyozawa *et al.,* J. Phys. Soc. Jpn. **48**, 472 (1980).
[8] M. Tanaka *et al.,* Chem. Phys. **96**, 343 (1985).
[9] S. Tomimoto *et al.,* Phys. Rev. B **60**, 7961 (1999).
[10] S. L. Dexheimer *et al.,* Phys. Rev. Lett. **84**, 4425 (2000).
[11] A. Shirakawa *et al.,* Appl. Phys. Lett. **74**, 2268 (1999).
[12] A. Sugita *et al.* (to be published).
[13] S. Tomimoto *et al.,* Phys. Rev. Lett. **81**, 417 (1998).
[14] R. J. H. Clark *et al.,* J. Chem. Soc. Dalton Trans. **1981**, 524 (1981).
[15] Y. Wada *et al.,* J. Phys. Soc. Jpn. **54**, 3143 (1985).
[16] A. Laubereau *et al.,* Rev. Mod. Phys. **50**, 607 (1978).
[17] Y. Yan *et al.,* J. Chem. Phys. **87**, 6240 (1987).